Article citation info:
FIEDKIEWICZ Ł, PIELECHA I. Assessment of possible use of the ionization signal for the combustion process diagnostics in a spark ignition combustion engine powered by natural gas. Eksploatacja i Niezawodnosc – Maintenance and Reliability 2018; 20 (4): 630–637, http://dx.doi.org/10.17531/ein.2018.4.14.

Łukasz FIEDKIEWICZ
Ireneusz PIELECHA

# ASSESSMENT OF POSSIBLE USE OF THE IONIZATION SIGNAL FOR THE COMBUSTION PROCESS DIAGNOSTICS IN A SPARK-IGNITION COMBUSTION ENGINE POWERED BY NATURAL GAS

# OCENA MOŻLIWOŚCI WYKORZYSTANIA SYGNAŁU JONIZACJI DO DIAGNOSTYKI PROCESU SPALANIA W SILNIKU SPALINOWYM O ZAPŁONIE ISKROWYM ZASILANYM GAZEM ZIEMNYM*

*The ionization signal, which is a result the presence of ions and electrons in the cylinder space of the internal combustion engine, is affected by many factors, including: temperature, pressure, fuel mixture composition, fuel type, presence of exhaust gases and others. The shape of the signal changes to a large extent from cycle to cycle, which indicates the stochastics of the combustion process. Nevertheless, its analysis provides a lot of useful information, such as the location of the maximum pressure or the maximum heat release rate. Using these signals allows supplementing the limited engine control systems of the combustion process in internal combustion engines. The paper presents a comparative analysis of the gas ionization current signal in the cylinder and the variable pressure at fixed operating points of a single-cylinder, four-stroke engine powered by natural gas. The analysis allowed to determine the relationship between the positions of the maximum thermal ionization signal value and of the maximum combustion pressure value. Additionally the relationship between the position of the maximum thermal fraction derivative and the maximum heat release rate was established.*

***Keywords***: *ionization sensor, engine control, engine diagnostics, indicated pressure, heat release.*

*Sygnał jonizacji wynikający z obecności jonów oraz elektronów w przestrzeni cylindra silnika spalinowego jest składową wielu czynników, między innymi: temperatury, ciśnienia, składu mieszanki, rodzaju paliwa, obecności reszty spalin oraz innych. Kształt sygnału zmienia się w znacznym stopniu z cyklu na cykl, co świadczy o stochastyce procesu spalania. Mimo tego, jego analiza dostarcza wielu przydatnych informacji, takich jak położenie maksymalnego ciśnienia czy maksymalnej szybkości wywiązywania się ciepła. Ich wykorzystanie pozwala uzupełnić ograniczone systemy kontroli procesu spalania w silnikach spalinowych. W artykule przedstawiono analizę porównawczą sygnału prądu jonizacji gazów w cylindrze oraz ciśnienia szybkozmiennego przy ustalonych punktach pracy jednocylindrowego, czterosuwowego silnika zasilanego gazem ziemnym. W wyniku analizy uzyskano zależność położenia maksymalnej wartości sygnału jonizacji termicznej od położenia maksymalnej wartości ciśnienia spalania, uzależniono również położenie maksimum pochodnej członu termicznego od położenia maksimum szybkości wywiązywania się ciepła.*

***Słowa kluczowe***: *czujnik jonizacji, sterowanie silnikiem, diagnostyka silnika, ciśnienie indykowane, wywiązywanie ciepła.*

## 1. Introduction

To assess the internal combustion engine combustion process validity, it is necessary to analyze the thermodynamic indicators, such as pressure, the start and end points of the combustion, the amount of heat released and the heat release rate. The most common way to obtain the above values is to measure the variable cylinder pressure of the engine and its further processing [12, 13, 16, 20]. In order to achieve this it is necessary to use pressure sensors that allow high sampling frequency measurements under high pressure and temperature conditions, and the same goes for the equipment communicating with the sensor. The costs of indicated systems limit their application to only scientific test engines and higher class vehicles. Optical systems are an alternative, available method [18, 19, 21] along with systems based on ionization current measurement in the cylinder [13, 15]. The analysis of a light wave requires using complicated apparatus, similarly as for the variable pressure indication [24]. The ionization current measurement has the widest application possibilities due to the system structure and low cost [4, 5, 8].

The primary purpose of ionization current measurement is to detect ignition failure and occurrence of knocking combustion [11]. These systems are characterized by a faster response time. There are also attempts to use the signal for multiple engine applications, such as: the measurement of the recirculated exhaust gas content in the air/fuel mixture [2, 14], assessment of excess air coefficient in the combusted fuel dose [22, 23], temperature measurement in the cylinder [9], ignition advance angle control with feedback in the form of information on the maximum combustion pressure location [10]. In recent years, research work has been performed to allow using the ionization signal for quality control and combustion control in CI engines running on a homogeneous mixture, also known as HCCI engines [1, 17].

As a result of ignition, the flame front propagates in the mixture from the spark plug electrodes towards the cylinder walls. The strong chemical reactions caused by these events sustain the process, thus

(*) Tekst artykułu w polskiej wersji językowej dostępny w elektronicznym wydaniu kwartalnika na stronie ***www.ein.org.pl*** leading to the production of ions and free electrons in the so-called chemical ionization phase. As a result of the increase of temperature and pressure in the final phase of the combustion process, the rate of ion formation significantly exceeds their recombination rate, which leads to an increase in their number. This phase is referred to as the thermal ionization phase.

Daniels [3] showed that the rate of ion formation is closely correlated with other significant thermodynamic combustion indicators, such as the ignition angle, the point of maximum flame front acceleration, the point of maximum heat release rate, the crankshaft angle of maximum pressure and the timing of the combustion process end. Eriksson [6] adds that the speed of the so-called the chemical ionization phase is closely related to the composition of the air-fuel mixture.

## 2. Ionization voltage signal

The measurement of ion number is performed using a spark plug, in the case of SI engines, or a sensor in CI engines. The idea is to create a large voltage potential difference (up to several hundred volts) between the spark plug electrodes, in the time period when the plug is not used to ignite the mixture (Fig. 1).

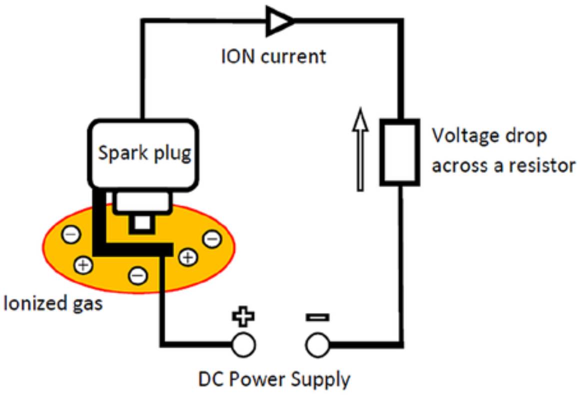


*Fig. 1. Diagram of the ionization signal measuring circuit [7]*

Due to the ability of ions and electrons to carry electric charge, a current flow appears (ionization current) proportional to the number of ions located in the vicinity of the electrodes. The measurement resistor, connected in series, has a potential difference proportional to the current of ionization according to the Ohm's law. This voltage is used directly by the measuring device and is referred to as the ionization voltage.

The characteristic ionization current signal has three distinct phases (Fig. 2):

a) ignition phase (210) – strong electromagnetic radiation from the ignition system – it causes interference in the ionization signal, making it difficult to analyze,
b) chemical ionization phase (220) – strongly associated with the emerging flame front,
c) thermal ionization phase (230) – is strongly dependent on the maximum pressure and temperature in the cylinder.

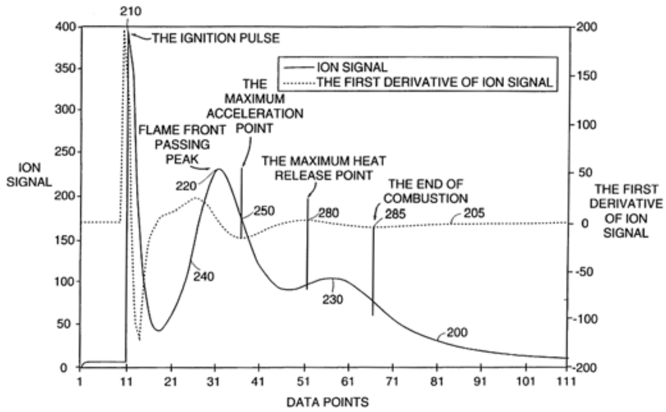


*Fig. 2. The ionization voltage signal and its first derivative with the three phases marked [3]*

In addition, the ion formation rate expressed as the first derivative of the ionization signal (205) contains the information regarding:

a) point of the maximum flame front acceleration (250) – inflection point occurring after the point of maximum chemical ionization; is the point of maximum flame acceleration, which signifies the end of ion formation in the vicinity of the spark plug electrodes (as a result of the flame front action as well as of further flame propagation into the combustion chamber),
b) the point of maximum heat release rate due to the mixture combustion process (280) – the local temperature around the spark plug increases with the intensity of the combustion process; thus, the ion formation rate in the thermal ionization phase in the vicinity of the spark plug is closely related to the heat release rate around the spark plug,
c) the end point of the combustion process (285) – the process of ion formation stops completely in the vicinity of the spark plug electrodes and the recombination intensity increases instead.

Due to the combustion process stochastics and the high sensitivity of the measurement method, the ionization current characteristics has a very low repeatability in relation to the cylinder pressure characteristic (Fig. 3a), which makes the signal analysis difficult (Fig. 3b). This is caused by the inability to ensure repetitive thermodynamic conditions and the required quality of the mixture in the space between the spark plug electrodes in each cycle of the engine's operation. This applies in particular to [6]:

a) the temperature – it affects the amount of energy provided for the ionization of molecules and the rate of ion recombination,
b) the air to fuel mass ratio – during the combustion of lean mixtures, the signal level decreases, which is caused by the lower combustion process temperature relative to the stoichiometric

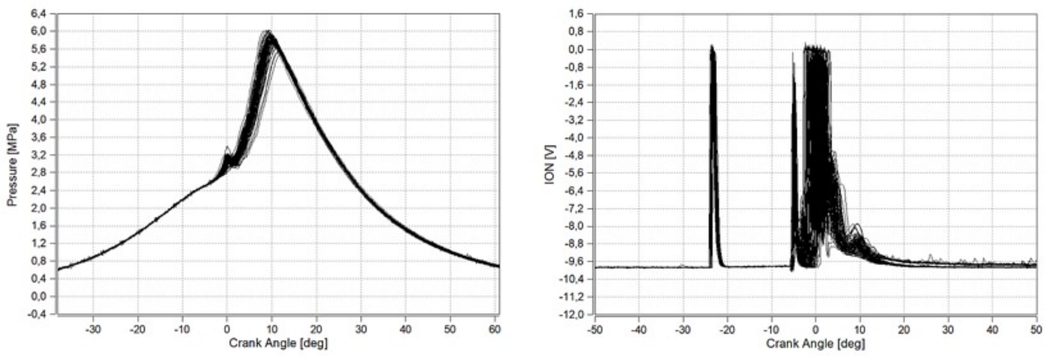


*Fig. 3. The non-repeatability of in-cylinder processes: a) combustion pressure, b) ionization voltage signal for 100 consecutive engine cycles (mean indicated pressure IMEP = 0.5 MPa, ignition start crankshaft angle = 6 deg before TDC, excess air ratio λ = 1)*

mixture; in addition, the lower density of fuel particles reduces the speed of flame front propagation, which again lowers the ion formation rate,

c) the fuel chemical composition – different types of fuels, depending on the arrangement of the hydrocarbon chains and the types of additives included, significantly affect the process of ions formation and recombination after ignition.

## 3. Aim of research

Usefulness of the ionization signal applies mainly to engines fueled with a stoichiometric gasoline mixture. There is little information in the literature on the subject of using this signal for combustion process diagnostics during the combustion of gas mixtures.

The aim of this research was to evaluate the possible use of the ionization signal for the diagnosis of thermodynamic processes occurring during the combustion of a fuel-air mixture where methane is used as the fuel. Such diagnostics will be deemed possible if the information it provides regarding the combustion conditions are sufficient to replace the cylinder pressure and the heat release rate characteristics with a diagnostic ionization signal. For this purpose, a comparative analysis of thermodynamic indicators was made, determined on the basis of the indicated pressure characteristics and the ionization voltage signal. The study attempted to establish relations between characteristic points of both methods and their location. Obtaining a correlation between the combustion process thermodynamic indicators and the ionization voltage signal will increase the diagnostic applicability of the signal, while allowing for greater combustion process control. Obtaining a correlation between these signals will also allow to eliminate additional sensors (e.g. combustion pressure), whose processing of the signal in real time in the engine control unit is challenging.

Analysis of the results of such tests will allow to extend the scope of diagnostics of internal combustion engines fueled not only with gasoline-air mixtures, but also with gaseous fuel mixtures.

## 4. Research methodology

### 4.1. Test object

The tests were performed on a single-cylinder four-stroke test engine marked as AVL 5804. The originally diesel-powered unit was modified to allow natural gas combustion. In order to achieve this, the injection system was modified (high-pressure direct injection was replaced by low-pressure indirect injection), the ignition system was installed and the compression ratio was reduced. The technical parameters of the test engine used are shown in Table 1.

### 4.2. Test bench

The tests were performed using specialized measuring equipment (Table 2) and dedicated control devices (Fig. 4). The ignition control (from Autoelektronika) enabled adjustment of the ignition advance angle and the discharge energy (function of charging time of the coil primary winding). An electronically controlled throttle was used to control the air intake. The electromagnetic natural gas injector from Bosch, controlled using the Autoelektonika company equipment, delivered the fuel dose at the specified crankshaft angle and for a specified injection duration. The pressure of the gas supplied from the high-pressure tank was regulated using a reducer and reached a level of 0.9 MPa. In order to limit wave phenomena, an additional volume of 2 $dm^3$ was installed in the natural gas supply system.

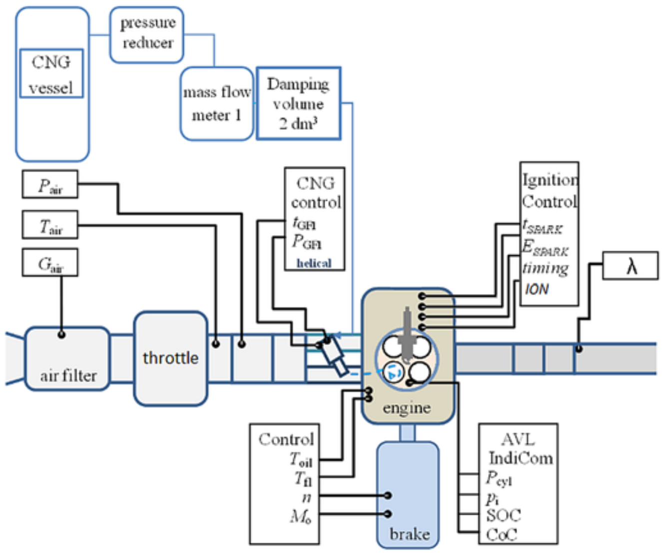


*Fig. 4. Ionization signal measurement test bench schematic [7]*

In order to maintain constant thermodynamic conditions, the stand was equipped with a liquid and oil conditioning system (constant temperature conditions of $T_{ol}$ = 80°C and $T_c$ = 80°C were maintained). A sensor integrated with the ignition coil, used in Mazda Skyactiv-G engines, was used to obtain the ionization voltage. The Kistler 6081A combustion pressure sensor was placed in the head of the test engine at a distance of 10 mm from the spark plug.

### 4.3. Scope of research

To determine the relationship between the combustion process thermodynamic indicators and the ionization signal, a test engine operating at a constant speed n = 1500 rpm and an excess air ratio λ = 1 was used. A constant initial value of the engine load in the form of indicated mean effective pressure IMEP = 0.43 MPa was assumed. This value was obtained with an ignition advance angle of 19 degrees before TDC. Fuel injection to the inlet channel was carried out at an

*Table 1. The AVL 5804 test engine technical data*

| Parameter | Unit | Value/type |
|---|---|---|
| Engine | – | 1-cylinder, 4-valves, SI |
| Displacement | $dm^3$ | 0.5107 |
| Diameter × stroke | mm | 85 x 90 |
| Compression ratio | – | 15.2 |
| Fuel system | – | Indirect gas injection (electromagnetic injector) |
| Air intake system | – | naturally aspirated engine |

*Table 2 . Apparatus used in the research*

| Parameter | Name | Measurement range |
|---|---|---|
| Engine dynamometer | AVL AMK DW13-170 | –50–300 Nm |
| Air intake rate | Sensycon Sensyflow | 0–720 kg/h |
| Fuel consumption | Bronkhorst 111B | 0.1–100 g/h |
| Lubrication system | AVL 577 | 0–150 °C |
| Cooling system | AVL 577 | 0–150 °C |
| Data acquisition system | AVL IndiSmart | 8-channel system |
| | AVL Concerto | Post-processing |
| Broadband oxygen sensor | Bosch LSU 4.9 | λ > 0.5 |

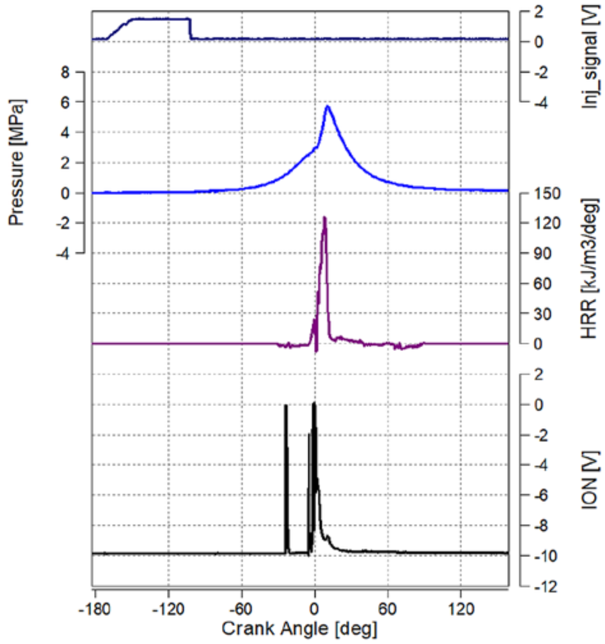


*Fig. 5. Indicator chart showing the analyzed parameters*

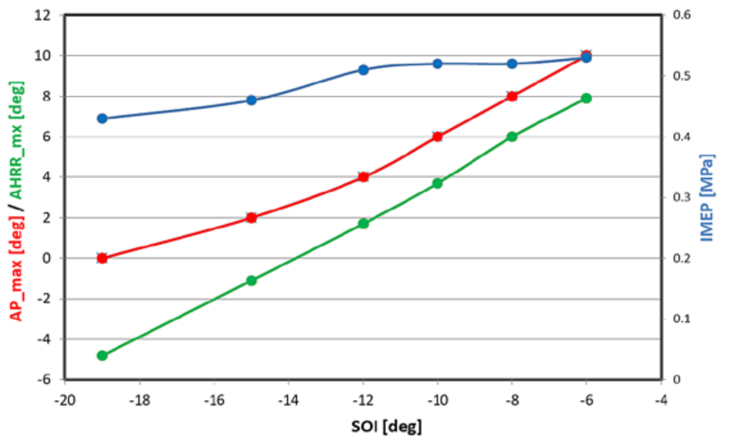


*Fig. 6. Influence of start of ignition angle on the averaged values of: indicated mean effective pressure (IMEP), maximum cylinder pressure angle (AP_max) and maximum heat release rate angle (AHRR_mx) in a natural gas engine (λ = 1)*

angle of 170 degrees before TDC. The fuel dose was kept constant at $q_o$ = 16.9 mg/injection. The ignition angle (SOI) was a variable. These conditions have caused a change in the combustion process. The indicated mean effective pressure (IMEP), the angle of maximum combustion pressure (AP_mx) and the angle of the maximum heat release rate (AHRR_mx) were analyzed further. The scope of research is shown in Table 3.

The combustion process data acquisition was performed with an angular resolution of 0.1 deg when registering 100 motor cycles, which were then averaged. The non-repeatability of the combustion process indicators was determined as the standard deviation σ from 100 measuring cycles; the resulting values (averaged from 100 cycles) are included in Table 3.

*Table 3. Test conditions and average resulting values*

| No. | Controlled variables | | | Resulting variables (average values) | | | | |
|---|---|---|---|---|---|---|---|---|
| | constant | | variable | | | | | |
| | n [rpm] | qo [mg/injection] | SOI [deg after TDC] | IMEP [MPa] | AP_mx [deg after TDC] | AHRR_mx [deg after TDC] | σ(AP_mx) [deg] | σ(AHRR_mx) [deg] |
| 1. | 1500 | 16.9 | −19 | 0.43 | 0 | −4.8 | 0.601 | 0.512 |
| 2. | | | −15 | 0.46 | 2 | −1.1 | 0.422 | 0.578 |
| 3. | | | −12 | 0.51 | 4 | 1.7 | 0.475 | 0.497 |
| 4. | | | −10 | 0.52 | 6 | 3.7 | 0.445 | 0.432 |
| 5. | | | −8 | 0.52 | 8 | 6.0 | 0.452 | 0.447 |
| 6. | | | −6 | 0.53 | 10 | 7.9 | 0.596 | 0.538 |

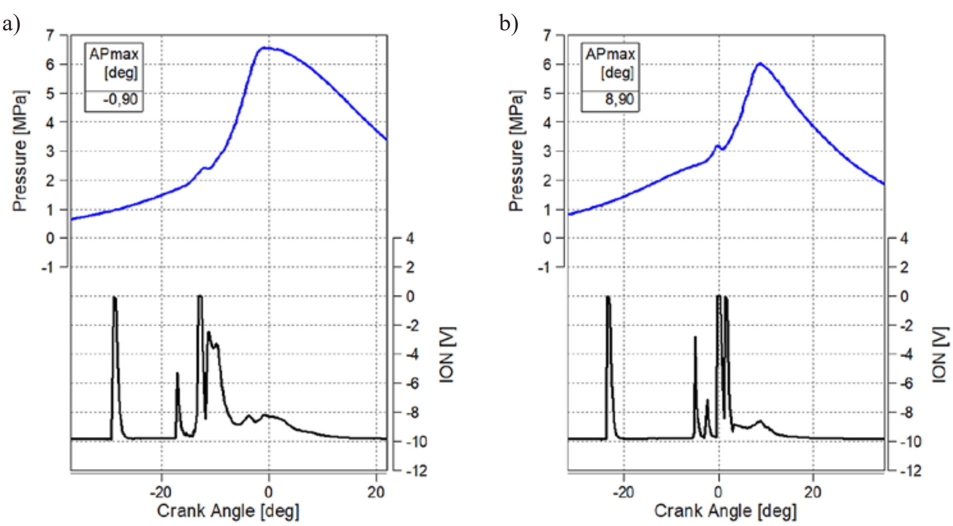


*Fig. 7. The indicated pressure and ionization voltage signal characteristics from the combustion chamber for extreme measuring points still within the scope of the tests: a) SOI = 19 deg before TDC, b) SOI = 6 deg before TDC*

The engine operating conditions shown in Table 3 were used to determine the relationship between the maximum combustion pressure point, the maximum heat release rate point and the ionization signal. Control signals along with the ionization signal and thermodynamic analysis results for an example non-averaged run are shown in Fig. 5.

Test conditions presented in Fig. 5 and Table 3 indicate that the change in the ignition timing angle settings directly affects the combustion process (with other engine operation parameters kept at constant values). As a result of the ignition delay the occurrence of the maximum combustion pressure, and then the angle of the maximum heat release rate are also delayed. Changes in these values are not proportional, which is shown in Fig. 6 for 100 averaged runs.

Due to the increase of the standard deviation value at the extreme start of ignition angle settings, the combustion pressure and ionization signal were analyzed at these operating points (Fig. 7). Data analysis shows that ignition of the mixture results in a characteristic pressure peak. This change corresponds to the other ionization signal characteristics in the combustion chamber.

The use of natural gas as a fuel required maintaining a stable engine operating temperature, due to its high impact on the conditions of the combustion process. Such conditions result from the low ther-

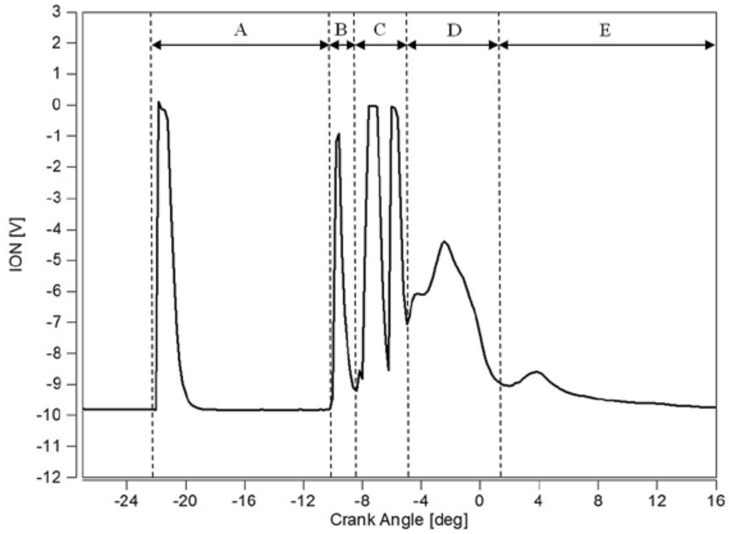


*Fig. 8. The real ionization voltage signal along with markers indicating the different phases*

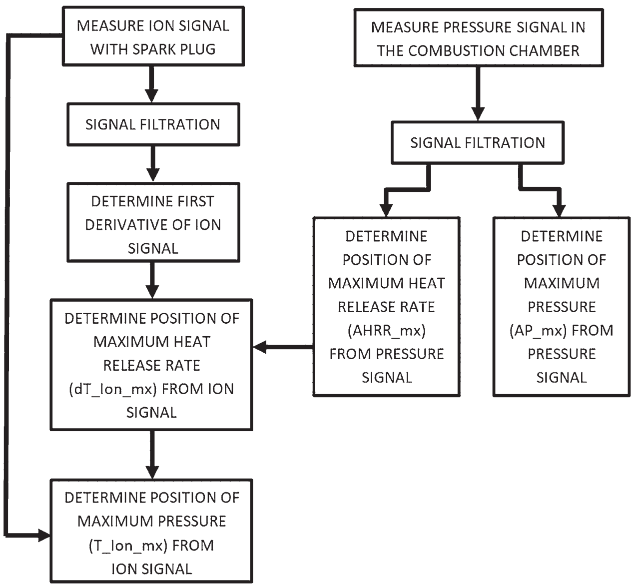


*Fig. 9. Calculation algorithm that allows to determine the characteristic points of the ionization signal and its derivative*

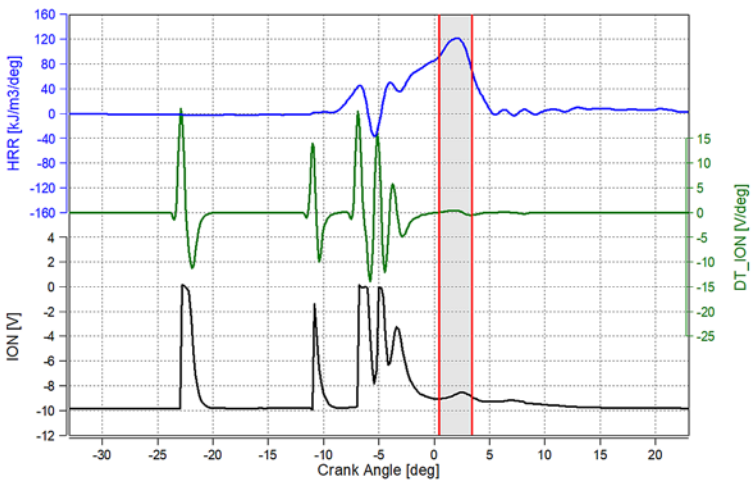


*Fig. 10. The ionization signal analysis range (3° on the crankshaft) – marked in red*

mal capacity of the natural gas as a fuel. The adopted temperature of 80°C was maintained by the liquid conditioning and oil conditioning systems.

## 5. Ionization signal test results analysis

### 5.1. Ionization signal characteristics

The obtained ionization voltage characteristics allow isolation of individual phases, both in the ignition phase and in the mixture combustion phase (Fig. 8). The first notable increase in the ionization voltage corresponds with the moment when the primary winding of the ignition coil starts charging. The duration of the charging phase (A) is limited by the second increase in the ionization signal that initiates the ignition phase (B). This phase results from the ignition coil finishing its charging process and the occurrence of the spontaneous induction phenomenon, which causes electric discharge of the spark plug on the electrodes. As a result of the discharge, the energy accumulated in the ignition coil is lost, resulting in the observed voltage oscillations on the secondary winding. They are reflected in the characteristic increases (C) of the ionization signal which make it difficult to measure the ionization current during the combustion process.

Analysis of the obtained ionization process characteristics in the combustion chamber indicates the existence of some discrepancies between the theoretical ionization signal and the real signal recorded. The real signal contains interference from the ignition system, which makes the analysis of the chemical ionization signal (phase D – Fig. 8) difficult. For this reason, further analysis of the ionization voltage signal concerns mainly its chemical part (phase E – Fig. 8).

This approach causes analyzes related to the ionization voltage signal to concern the combustion process, not the evaluation of the pre-flame processes. The result is that such a signal will be used to evaluate the combustion process, not to assess the timing of ignition or to estimate other quantities (such as the excess air ratio) before ignition in the vicinity of the spark plug.

### 5.2. Algorithm for determining the process indicators

To find the correlations (presented in chapter 3) a program was created (using the AVL Concerto software) to determine the characteristic points of the ionization signal (chapter 2). Using this calculation algorithm (Fig. 9), in the first stage, the ionization signal and pressure signal were filtered with a low-pass filter. Next, the first derivative (dT_Ion) was determined containing information about the angular position of the maximum heat release rate. The maximum heat release rate value obtained using the pressure characteristic (AHRR_mx) made it possible to limit the ionization signal analysis to within 3-degrees on the crankshaft. In this respect, the algorithm determined the maximum ionization signal value and its derivative (Fig. 10).

The selected range of ±1.5 degrees on the crankshaft in relation to the maximum heat release rate value location determined by using the pressure values, proved highly efficient in determining the characteristic points of the ionization signal (T_Ion_mx) and its derivative (dT_Ion_mx).

### 5.3. The relation between the ionization signal and the thermodynamic indicators of the combustion process

To determine the relationship between the ionization voltage signal and the thermodynamic indicators of the combustion process (obtained from the cylinder pressure signal) and the heat release rate, the focus was placed on their characteristic values:

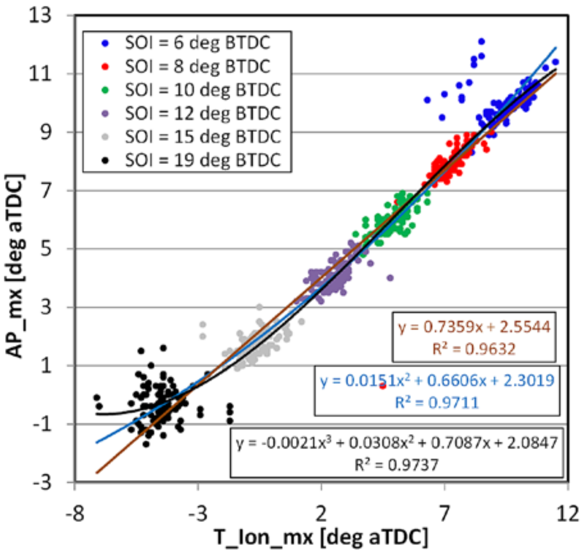


*Fig. 11. The relation of the maximum pressure angle (AP_mx) and the maximum value of the thermal ionization voltage angle (T_Ion_mx) including all test points*

a) angular position at the maximum cylinder pressure – AP_mx [deg]; this quantity was obtained through indication,
b) the angular position at the maximum heat release rate – AHRR_mx [deg]; this size was obtained using the equation:

$$\frac{AHRR\_mx}{d\alpha} = \frac{\kappa}{\kappa-1}\left(\frac{P_\alpha + P_{\alpha+1}}{2}\right)\left(V_{\alpha+1} - V_\alpha\right) + \frac{1}{\kappa-1}\left(\frac{V_\alpha + V_{\alpha+1}}{2}\right)\left(P_{\alpha+1} - P_\alpha\right)$$

where:

- P – cylinder pressure,
- V – volume above the piston,
- κ – politropic compression and expansion factor (κ = 1.32),the indexes α and α+1 indicate the current and next crankshaft angle value.

c) angular position at the maximum ionization voltage value in the thermal phase – T_Ion_mx [deg]; this value was obtained

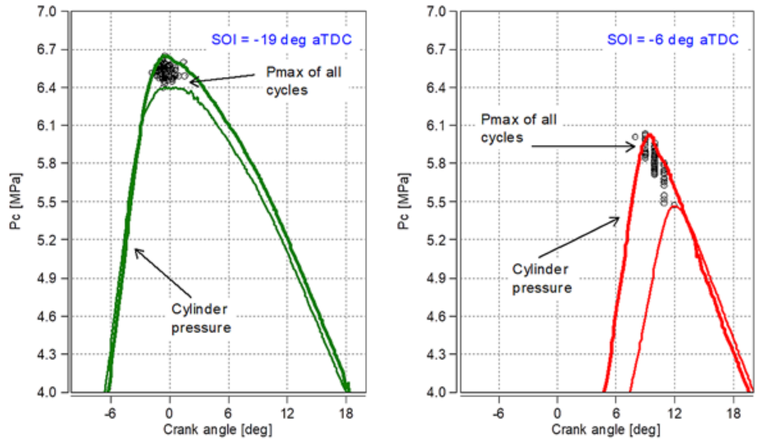


*Fig. 12. Changes in the AP_mx angle value at the extreme ignition angle (SOI = 19 before TDC and 6 deg before TDC)*

using the ionization sensor (Fig. 1) and the designed algorithm (chapter 5.2),
d) the angular position at the maximum derivative value of the thermal phase ionization signal – dT_Ion_mx [deg]; this size was obtained using the designed algorithm.

The analysis of the relationships between the values of AP_mx and T_Ion_mx as well as AHRR_mx and dT_Ion_mx reveals that it is possible to make a comparison between them and thus search for correlation. The analysis of the relationship between the maximum pressure crankshaft angle and the maximum value of the thermal ionization signal angle indicates a large correlation of these values with all the research points (Fig. 11).

These correlations are presented in relation to the linear function, quadratic and third order functions (logarithmic and exponential functions were not used due to the presence of negative values of both variables). Their determination coefficients have a similar value of 0.97. The differences between them are within 3%. This means that it is possible to adopt a linear function to determine the maximum cylinder pressure angle value based on the ionization signal. This function is also more useful in the implementation of such a solution, because it allows to increase the speed at which the AP_mx value can be de-

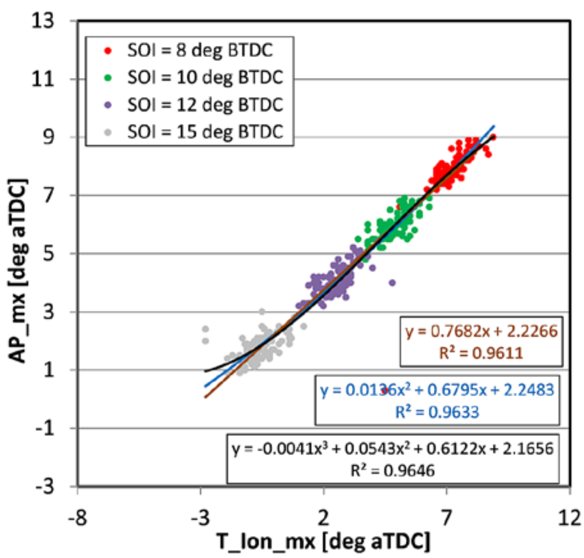


*Fig. 13. The relation between the maximum pressure angle (AP_mx) on the crankshaft angle at the maximum thermal ionization voltage (T_Ion_mx) after reducing the number of test points*

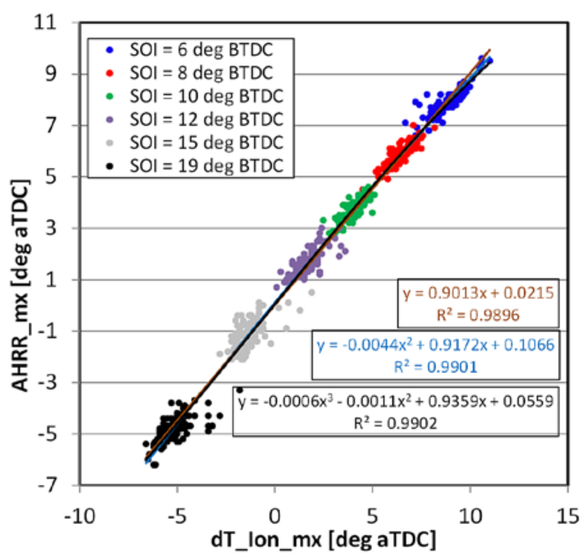


*Fig. 14. The relation between the angle at maximum heat release rate (AHRR_mx) and the angle at the maximum derivative of the thermal phase (dT_Ion_mx) for all test points*

termined in the engine controller in real time (shorter calculation time using a specific algorithm).

However, for extreme ignition timing values (SOI = 19 deg before TDC and 6 deg before TDC), large discrepancies in cylinder pressure were observed. This results in a significant variation in the angle value at the maximum cylinder pressure (Fig. 12). The measure of this dispersion (indicator) are the values of standard deviation σ(AP_mx) of 0.601 deg and 0.596 deg respectively. They are the largest values of standard deviation when compared to other research points (Table 3). As a result, the correlation between the AP_mx and T_Ion_mx signals diminishes for the extreme values of SOI.

Taking into account the above analyzes forced a limitation of the data range used to determine the relationship between AP_mx and T_Ion_mx signals, the criterion for selecting test points was that the value of standard deviation had to be below 0.5 deg. This limitation therefore requires not taking into account the extreme values of the start of ignition angle. The results of such analyzes are presented in Fig. 13.

The analysis of the results from Fig. 13 indicates the achievement of determination coefficients at the level of 0.96 (within the margin of error of 1%). It follows that it is possible to take into account a limited number of measurement data and adopt the linear relation of the function AP_mx = f(T_Ion_mx) for them. The determination coefficient of 0.9611 and the standard deviation σ(AP_mx) below 0.5 deg guarantee that the condition of linearity of these variables is met.

The analysis of the function AP_mx = f(T_Ion_mx) indicates the possibility of correlation between these variables considering only the standard deviation of the maximum cylinder pressure angle below 0.5 deg. This means that in order to obtain a specific correlation of these variables it is necessary to determine the above standard deviation and to adopt the criterion of its upper value limit.

The analysis of the relation between the angle at the maximum heat release rate (AHRR_mx) and the angular position of the maximum value of the thermal phase derivative (dT_Ion_mx) indicates a highly linear relationship (Fig. 14) for all the test points. In this case, the linear, quadratic and tertiary functions were also determined. For all of these considerations, the obtained determination coefficients are similar and the discrepancies are below 0.1%.

The obtained values of standard deviation σ(AHRR_mx) below 0.6 deg enable using all of the research points to determine the relationship between the values of AHRR_mx and dT_Ion_mx.

The determination coefficients for the function AHRR_mx = f(dT_Ion_mx) show a high correlation of thermodynamic signals with ionization voltage signals, for all test points. The higher value of the maximum heat release rate angle is linearly dependent on the angle at the maximum thermal ionization phase derivative value. Due to the lack of significant differences in the determination coefficients, using a linear relationship was proposed, since it can allow for faster determination of the thermodynamic indicators (angle at the maximum heat release rate) in real time.

Analysis of the standard deviation of both these relations indicates that the correlations obtained using a standard deviation below 0.6 deg are valid. Accepting the deviation AP_mx with a value of 0.596 deg (SOI = 6 deg before TDC) indicates the existence of a limited correlation. Adopting the deviation AHRR_mx with a value of 0.578 deg still allows to obtain a good correlation. Such small differences in standard deviations mean that further tests may be necessary to precisely specify the numerical criterion and limit values for determining the correlation of these variables.

The analyzes presented above indicate the possibility of replacing the selected thermodynamic engine performance indicators with ionization voltage signals, which are possible to achieve with much simpler methods than their thermodynamic counterparts.

## 6. Conclusions

The analysis of the test results indicates the possibility of using the ionization voltage signal to diagnose the combustion process of the spark-ignition engine powered by natural gas with the excess air ratio of $\lambda = 1$.

The performed tests and analyses have shown that:

1. There is a strong relationship between the angle at the maximum thermal ionization signal value and the angle at maximum combustion pressure – the determination coefficient is $R^2 = 0.9611$. However, this relationship makes it possible to reproduce the angle of maximum combustion pressure based on the ionization voltage signal using a linear (proportional) relationship between signals only in a limited range of the ignition advance angle (8-15 degrees before TDC).
2. There is a strong relationship between the angle at the maximum thermal phase derivative value and the angle at the maximum heat release rate – the determination coefficient is $R^2 = 0.9896$, when using all the research points. This dependence makes it possible to determine the crankshaft angle at the maximum heat release rate based on the ionization signal value by adopting a linear (proportional) relationship between the two signals.
3. It is necessary to precisely determine the criteria for the operation of the internal combustion engine in order to obtain a high correlation of these signals. The standard deviation value limit used in the previous analyzes may be one of such criteria.

The obtained research results indicate that there is some merit to using the ionization signal in modern diagnostic systems for gasoline-powered internal combustion engines and their control systems. The ionization signal obtained in each combustion engine cycle – strongly correlated with the cylinder pressure and the heat release rate characteristics – allows a precise control of the indicated parameters, contributing to a quick detection of incorrect cycles and improvement of the combustion engine performance indicators.

Further research on this subject will focus on the possibility of extending the applications of the ionization signal to include all other test points and eliminating the information noise associated with the electric discharge on the spark plug, which will also enable the diagnosis of the pre-flame phase of the combustion process (chemical ionization phase). The solution to this problem will allow to expand the applications of the ionization signal by measuring the quality of the air-fuel mixture, as well as to measure the temperature in the cylinder. These research results can significantly contribute to improving the combustion process control in order to improve the performance indicators of spark-ignition engines fueled with natural gas and, in result, to reduce the emission of toxic compounds.

**Acknowledgements**

*The research presented in the article was conducted as part of the statutory work nr 05/52/DSPB/0261.*

## References

1. Butt R H, Chen Y, Mack J H, Saxena S, Dibble R W, Chen J Y. Improving ion current of sparkplug ion sensors in HCCI combustion using sodium, potassium, and cesium acetates: Experimental and numerical modeling. Proceedings of the Combustion Institute 2014; 35(3), doi: 10.1016/j.proci.2014.06.084.

2. Byttner S, Holmberg U. Closed-loop control of EGR using ion currents. Proceedings of the 27th IASTED International Conference Modelling, Identification and Control 2008; 978-0-88986-711-6.
3. Daniels C F. Mass fraction burned and pressure estimation through spark plug ion sensing. Patent US 6089077 A (2000).
4. Dev S, Sandhu N S, Ives M, Yu S, Zheng M. Ion current measurement of diluted combustion using a multi-electrode spark plug. SAE Technical Paper 2018; 2018-01-1134, doi:10.4271/2018-01-1134.
5. Dong G, Chen Y, Wu Z, Li L, Dibble R. Study on the phase relation between ion current signal and combustion phase in an HCCI combustion engine. Proceedings of the Combustion Institute 2015; 35 (3): 3097–3105, https://doi.org/10.1016/ j.proci.2014.08.033.
6. Eriksson L. Methods for ionization current interpretation to be used in ignition control. Diploma Thesis 1995.
7. Fiedkiewicz Ł, Pielecha I, Wisłocki K. Use of the gas ionization signal for combustion process diagnostics in the cylinder of a spark ignition engine. Combustion Engines 2017; 171 (4): 196-200, doi: 10.19206/CE-2017-433.
8. Filipek P, Wendeker M, Kamiński T, Mitraszewska I, Nowacki G. Opinion of ionization signal to estimating composition of mixture in combustion process about engine SI. Journal of KONES Powertrain and Transport 2008; 15 (3): 121–127.
9. Gao Z, Wu X, Man C, Meng X, Huang Z. The relationship between ion current and temperature at the electrode gap. Applied Thermal Engineering 2012; 33–34: 15–23, https://doi.org/10.1016/j.applthermaleng.2011.07.014.
10. Hellring M, Holmberg U. An ion current based peak-finding algorithm for pressure peak position estimation. SAE Technical Paper 2000; 2000-01-2829, https://doi.org/10.4271/2000-01-2829.
11. Hung D, Zhu G, Danne N, McKoskey J. Knock detection for a large displacement air-cooled V-twin motorcycle engine using in-cylinder ionization signals. SAE Technical Paper 2008; 2008-32-0028, https://doi.org/10.4271/2008-32-0028.
12. Koszałka G. Model of operational changes in the combustion chamber tightness of a diesel engine. Eksploatacja i Niezawodnosc – Maintenance and Reliability 2014; 16 (1): 133–139.
13. Kruczyński S, Ślęzak M, Gis W, Orliński P. Evaluation of the impact of combustion hydrogen addition on operating properties of self-ignition engine. Eksploatacja i Niezawodnosc – Maintenance and Reliability 2016; 18 (3): 343–347, http://dx.doi.org/10.17531/ein.2016.3.4.
14. Kusuhara T, Shinkai T, Yoshida K, Langley D. Development on internal EGR feedback control based on ion current. SAE Technical Paper 2017; 2017-01-0793, doi:10.4271/2017-01-0793.
15. Lagana A A M, Lima L L, Justo J F, Arruda B A, Santos M M. Identification of combustion and detonation in spark ignition engines using ion current signal. Fuel 2018; 227: 469–477, doi: 10.1016/j.fuel.2018.04.080.
16. Mikulski M, Wierzbicki S, Piętak A. Zero-dimensional 2-phase combustion model in a dual-fuel compression ignition engine fed with gaseous fuel and a divided diesel fuel charge. Eksploatacja i Niezawodnosc – Maintenance and Reliability 2015; 17 (1): 42–48.
17. Phan T, Mack J H, Butt R H, Dibble R. A comparison of three ion sensing circuits in a homogeneous charge compression ignition engine. Combustion Science and Technology 2017; 189 (8), https://doi.org/10.1080/00102202.2017.1294587.
18. Pielecha I, Pielecha J, Skowron M, Mazanek A. The influence of diesel oil improvers on indices of atomisation and combustion in high-efficiency engines. Polish Maritime Research 2017; 24 (3): 99–105, http://doi.org/10.1515/pomr-2017-0094.
19. Pielecha I, Skowron M, Mazanek A. Evaluation of the injectors operational wear process based on optical fuel spray analysis. Eksploatacja i Niezawodnosc – Maintenance and Reliability 2018; 20 (1): 83–89, http://dx.doi.org/10.17531/ein.2018.1.11.
20. Pielecha I, Wisłocki K, Cieślik W, Bueschke W, Skowron M, Fiedkiewicz Ł. Application of IMEP and MBF50 indexes for controlling combustion in dual-fuel reciprocating engine. Applied Thermal Engineering 2018; 132: 188–195, http://dx.doi.org/10.1016/j.applthermaleng.2017.12.089.
21. Piernikarski D, Hunicz J, Komsta H. Detection of knocking combustion in a spark ignition engine using optical signal from the combustion chamber. Eksploatacja i Niezawodnosc – Maintenance and Reliability 2013; 15 (3): 214–220.
22. Rao R, Honnery D. A simplified mechanism for the prediction of the ion current during methane oxidation in engine-like conditions. Combustion and Flame 2015; 162 (7): 2928–2936, https://doi.org/10.1016/j.combustflame.2015.03.011.
23. Rivara N, Dickinson P B, Shenton A T. A transient virtual-AFR sensor using the in-cylinder ion current signal. Mechanical Systems and Signal Processing 2009; 23 (5): 1672–1682, https://doi.org/10.1016/j.ymssp.2009.01.004.
24. Wendeker M. Sterowanie wtryskiem w silniku samochodowym. Lublin: Lubelskie Towarzystwo Naukowe, 1999.



**Łukasz FIEDKIEWICZ**
**Ireneusz PIELECHA**
Institute of Combustion Engines and Transport
Poznan University of Technology
Piotrowo 3, 60-965 Poznan, Poland

E-mails: Lukasz.M.Fiedkiewicz@doctorate.put.poznan.pl, Ireneusz.Pielecha@put.poznan.pl